

# A Hierarchical Poisson Generator for Universal Graphs under Limited Resources

Xiaorui Qi  
College of Computer Science  
Nankai University  
Tianjin, China  
qixiaorui@mail.nankai.edu.cn

Yanlong Wen\*  
College of Computer Science  
Nankai University  
Tianjin, China  
wenyl@nankai.edu.cn

Xiaojie Yuan  
College of Computer Science  
Nankai University  
Tianjin, China  
yuanxj@nankai.edu.cn

**Abstract**—Graph generation is one of the most challenging tasks in recent years, and its core is to learn the ground truth distribution hiding in the training data. However, training data may not be available due to security concerns or unaffordable costs, which severely blows the learning models, especially the deep generative models. The dilemma leads us to rethink non-learned generation methods based on graph invariant features. Based on the observation of scale-free property, we propose a hierarchical Poisson graph generation algorithm. Specifically, we design a two-stage generation strategy. In the first stage, we sample multiple anchor nodes according to the Poisson distribution to further guide the formation of substructures, splitting the initial node set into multiple ones. Next, we progressively generate edges by sampling nodes through a degree mixing distribution, adjusting the tolerance towards exotic structures via two thresholds. We provide theoretical guarantees for hierarchical generation and verify the effectiveness of our method under 12 datasets of three categories. Experimental results show that our method fits the ground truth distribution better than various generation strategies and other distribution observations.

**Index Terms**—Graph Generation, Graph Algorithm, Hierarchical Modeling, Power-law Distribution

## I. INTRODUCTION

Graph generation task, widely used for scenarios like social analysis [1]–[3], molecule generation [4]–[6], and structure modeling [7]–[9], is one of the hottest researches in recent years. Maintaining the distribution similarity between the generated and ground truth graphs is the core and one of the challenges of this task. Deep Generative Models (DGM) are the mainstream solutions nowadays [10], [32], [49]–[51]. DGM learns the latent distribution features hiding in the training data, generating graphs closer to the requirements.

However, training data may not be available due to security concerns or high data acquisition costs [13], striking learning models severely, especially DGM. Figure 1 illustrates this limitation. Only plain graph property data, such as the number of nodes and edges, are available when we limit the training data. The learnable distribution space of DGM switches from the training set to the search space of node permutations, resulting in the generation of mess graphs out of distribution (in red). Some studies have proposed solutions to this problem, such as graph transfer learning [11]–[13], which realizes graph generation in restricted scenarios by learning invariant features

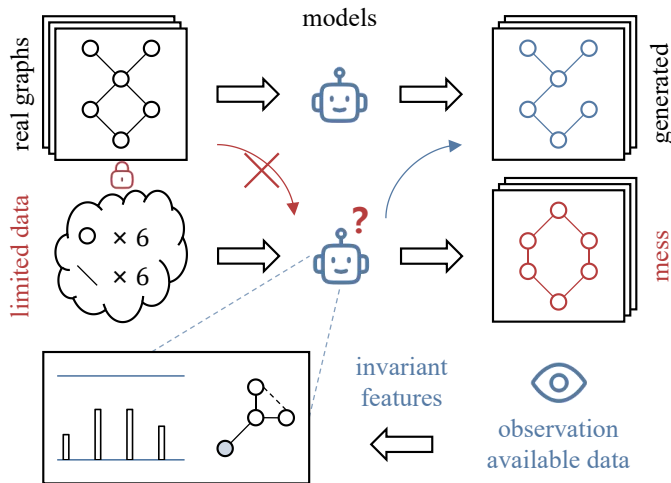


Fig. 1. An illustration of deep learning models with limited/no training data failing to generate graphs due to safety propose or high price (in red). However, with invariant features dragging from observation on universal data available, we can generate graphs fitting ground truth distribution well without learning (in blue).

in other training data that can be easily obtained. Nevertheless, the quality of such solutions depends heavily on the quality of the training data before transfer. There is heterogeneity in the data distribution of different scenarios [14]. The model performance is unsatisfactory if there are considerable differences in the invariant features. For example, social networks have many clusters, while molecules rely on functional groups with unique semantics. Models can not learn sufficient invariant features transferring one scene above to another. Improving the quality of training data further increases the acquisition cost, returning to the previous limitations.

This dilemma urges us to rethink non-learned generation methods based on graph invariant features. Throughout the history of graph generation tasks, traditional methods have been designed on universal observations maintained in real-world scenarios, such as randomness [44], small world [46], scale-free [36], [40], [45], etc. These observations are equal to invariant features independent of the training data, satisfying the properties of graphs under most scenarios. Among them,

\* Yanlong Wen is the corresponding author.

we pay attention to the scale-free property of graphs. Scale-free, also known as power-law, heavy-tailed, etc., refers to a phenomenon in which a small number of nodes in networks have a large number of connections, while most nodes have only a few. Many systems in the real world have this property [34], [45], reflected in the distribution of various aspects, such as degree, label, resources, etc. It will serve as a significant invariant feature observation that effectively organizes the basic graph information to direct the generation.

But, instead of DGM learning the real-world distribution accurately, a selected invariant feature often orients to a class of graph sets with its hand-crafted characteristics. For example, Chung-Lu (CL) [40] generates strictly scale-free networks and does not perform well in generating other graphs that do not follow this degree distribution. R-MAT [36], a scale-free graph generator based on an iterative strategy, creates graphs primarily depending on the initial graph. Some more methods [37], [38], [47] serve the corresponding set of graphs depending on the user-defined feature constraints, while others [15]–[17] define particular scenarios, leaving the decision to randomness. When learning approaches are limited as a resource, the unapproachable power of predefined features kills the generalization ability of non-learned methods [34]. Therefore, whether enhancing the generality of invariant features or weakening selected features by noises, restrictions, etc., can improve the support of non-learned methods for rich graph categories.

We further reinforce the limited resources problem setting with real-world scenarios. On the one hand, the training data may be constrained. For example, users’ relationships have semantics [23] (e.g., motifs [18]). In this case, it is not enough to provide basic data anonymization. The implicit distribution patterns are leaked if the training data is available, causing severe security problems. On the other hand, learning approaches may be limited. For example, there is insufficient data and resources with quantity and quality assurance in some marginal application scenarios to support model learning. In addition, due to the black-box nature of the learning model, the learned invariant features do not have good interpretability.

Admittedly, generating graphs relying entirely on basic information such as the number of nodes and edges is tantamount to randomly selecting from the search space. DGM mainly obtains real-world distribution through feature matrix [19]–[22], node sequence [23], [24], etc., while some extend the sampling space by mixup through the semantic information of specific scenes [25]–[27]. These models are training data available, and the ground truth distribution is known. How to use as little additional information as possible without breaking the limited resources is also a vital consideration in designing a generation strategy for universal graphs. For example, Erdős-Rényi (ER) [44], the most typical random graph model, only employs the number of nodes and a uniform probability of edge generation. Barabási-Albert (BA) [45] gradually generates the edges in the graph based on the preferential attachment, including three parameters: the initial graph, the number of nodes, and the number of coming

edges for new nodes.

Overall, to devise graph generation methods under limited resources scenarios, we have the following challenges: **(1) Capture powerful invariant features.** The ground truth distribution cannot be learned directly due to the difficulty of obtaining training data. We need a generation strategy based on a powerful invariant feature covering the majority of scenes. **(2) Weaken the influence of manual design.** Traditional methods are engineered for a family of graphs with selected features, leading to poor scalability [34]. We need to weaken the influence of particular features to support the generation of diverse structures. **(3) Generate graphs that fit the ground truth distribution.** The effect of invariant feature selection will eventually be reflected in the distance evaluation between the generated and real-world graphs. We need to generate graphs closer to the ground truth.

To solve the above problems, we propose a hierarchical Poisson graph generation algorithm, which generates universal graphs under the observation of the scale-free property. Specifically, we design a two-stage generation strategy. In the first stage, we sample a set of anchor nodes based on the Poisson distribution to further guide the formation of substructures, splitting the node set into multiple ones. It corresponds to challenge 1, where we strictly follow scale-free invariant features for graph generation. In the second stage, we employ preferential attachment to weight the Poisson distribution to alleviate the feature limitations mentioned in challenge 2. We progressively generate the remaining edges by sampling node pairs through a degree mixing distribution. Finally, facing challenge 3, we leverage two basic graph information as thresholds to adjust the algorithm tolerance for generating exotic structures and further enrich the search space well-fitted to ground truth distribution. We provide theoretical underpinning that guarantees that the generative process is interpretable.

In summary, our contributions are as follows:

- We explore the possibility of generating graphs in the setting of limited resources and rethink the generation strategy only through basic graph properties.
- We design a hierarchical Poisson generator based on the scale-free property for universal graphs under limited resources, which creates graphs closer to the real-world distribution.
- We provide theoretical guarantees for our method and design a fast version in a pairwise perspective, achieving a balance between performance and efficiency.
- Experiments on 12 datasets in three categories give a thorough perspective to evaluate our work. Results show that our method can cover most scenarios when the ground truth distribution is unknown.

## II. RELATED WORK

In this section, we systematically review the graph generation tasks. It has a long development history, briefly separated into traditional methods and deep generative models based on

time. Finally, we briefly introduce methods based on transfer learning.

### A. Traditional Methods

In the early stage, traditional graph generation methods rely on human-made characteristics or particular strict constraints. Erdős-Rényi (ER) [44] and Watts-Strogatz (WS) [46] are the most famous graph generation paradigms. The former is  $\mathcal{G}_{np}$ , where  $n$  is the number of nodes and  $p$  is the connection probability between every node pair. The latter is  $\mathcal{G}(n, k, p)$ , which requires that each node associates with its  $k$  neighbors at initialization. Then, one of the endpoints of each edge will change with probability  $p$ . The graphs created by ER have a low clustering coefficient and do not have the properties of real-world graphs. WS overcomes this and maintains properties like high clustering and small world but may produce unrealistic degree distribution. Barabási-Albert (BA) [45] pays attention to the preferential attachment phenomenon, defines  $p$  as the degree proportion where  $p_u = \frac{d_u}{\sum_{v \in \mathcal{N}(u)} d_v}$ , and proposes a progressive generation method that gradually adds nodes. Therefore, BTER [37] created a hierarchical generation method combining ER and BA, leveraging the node proportion to connect multiple ER pre-generated graphs.

Similar to hierarchy, another branch of recursive generation exists. These methods generate graphs from an initial graph  $\mathcal{G}_0$ . R-MAT [36] and Kronecker [48] notice the adjacency matrix, creating self-similarity graphs by copying the initial one. Meanwhile, Mixed-Membership Stochastic Block (MMSB) [47] shares the same idea of parsing graphs into multiple blocks as BTER, which builds a reliable community analysis. In summary, traditional methods can generate graphs within a particular pattern with small amounts of graph statistical parameters, guaranteeing robust interpretability.

### B. Deep Generative Models

Considering the limitations of traditional methods, researchers have shifted their attention to Deep Generative Models (DGM) in recent years. Depending on the technique employed, DGM can be divided into four categories: Variational Auto-Encoders (VAE) [28], Generative Adversarial Networks (GAN) [29], Normalizing Flows (NF) [30], and Diffusion models [31]. VAE and NF transform the original graph feature space into a low-dimensional vector, where the former leverages a well-trained Graph Neural Network (GNN) based encoder and decoder, and the latter uses a sequence of invertible functions. GAN implicitly learns the distribution of the original graph by training a pair of generators and discriminators, which play against each other. Denoising diffusion models originated from the field of computer vision. The core idea is to perturb the original distribution through a designed noise model and then train a learnable denoising process to recover the original graph data from the noise.

We use an earlier contemporaneous GraphRNN [49], which leverages recurrent neural networks as the backbone, to represent the single class of technical schemes. Meanwhile, the majority of popular DGM uses a mixed architecture. For

TABLE I  
NOTATIONS AND DEFINITIONS.

Symbols	Definition & Description
$\mathcal{G}$	Graphs
$\mathcal{V}, \mathcal{E}$	Set of nodes and edges
$N, M$	Number of nodes and edges
$(N, M)$	A graph with $N$ nodes and $M$ edges
$\bar{D}, d_{max}$	Average and maximal degree
$d_u$	Degree of node $u$
$P(\lambda)$	$\lambda$ -Poisson Distribution
$P(k_0 \lambda)$	$\lambda$ -Poisson Distribution when $X = k_0$
$k$	Minimum positive integer satisfying $P(k \lambda) < P(0 \lambda)$
$\mathcal{G}_{sub}$	Sequence of substructures
$v_0^{(i)}$	Anchor node of $\mathcal{G}_{sub}^{(i)}$
$D$	Degree sequence of anchor nodes
$L_{ent}$	Entry list, where $L_{ent}[i][j]$ is the degree of node $v_j^{(i)}$
$Pr(\cdot)$	Node selection probability
$s_{sub}^{(i)}$	Node proportion of $\mathcal{G}_{sub}^{(i)}$
$P_E, P_e$	Edge selection probability
$c$	Graph sparsity

example, GraphARM [50] relies on an autoregressive diffusion scheme to improve the generation speed of a single solution. GraphILE [51] designs the pipeline based on graph coarsening and expansion techniques and integrates the denoising process for training. CatFlow [32] introduces variational inference to flow matching, amplifying the advantages of both. In short, DGM learns the probable graph distribution from the training data and then guides the following generation. For more details on the graph generation tasks, please refer to [33]–[35].

### C. Graph Transfer Learning

Graph transfer learning aims to learn the knowledge of the source domain and apply it to the target domain to improve the model performance. HyRel [13] introduces intrinsic hyperrelation structures as invariant features to achieve global transferability and guide inductive link prediction on unseen graphs. With the help of an external urban knowledge graph, ADAPTIVE [12] uses a feature-enhanced generative adversarial network to generate cellular traffic in the city without historical traffic data. TGG [11] inversely uses graph generation to explicitly model unseen relationships, contributing to zero-shot and few-shot learning by capturing multi-granularity relationships through the aggregation network based on attention mechanism. However, the target domain in graph transfer learning is usually sparse graph samples or under-labeled, which is different and weaker in constraints from the limited resources problem setting in this paper.

## III. PRELIMINARY

We start with the definition of the graph.

*Definition 1 (Graph):* A graph can form as  $\mathcal{G} = \{\mathcal{V}, \mathcal{E}\}$ , where  $\mathcal{V}$  and  $\mathcal{E}$  represent nodes and edges set, and  $N$  and  $M$  are the number of nodes the edges, respectively.  $A[u, v] \in \{0, 1\}^{N \times N}$ ,  $u, v \in \mathcal{V}$  is the adjacency matrix, where  $A[u, v] = 1$  shows there is an edge between node  $u$  and node  $v$ . We use  $d_u$  to represent the degree of node  $u$ . For an undirected graph,  $d_u = \sum_{v \in \mathcal{V}} A[u, v]$ . We use  $(N, M)$  as a shorthand for a graph  $\mathcal{G}$  with  $N$  nodes and  $M$  edges.

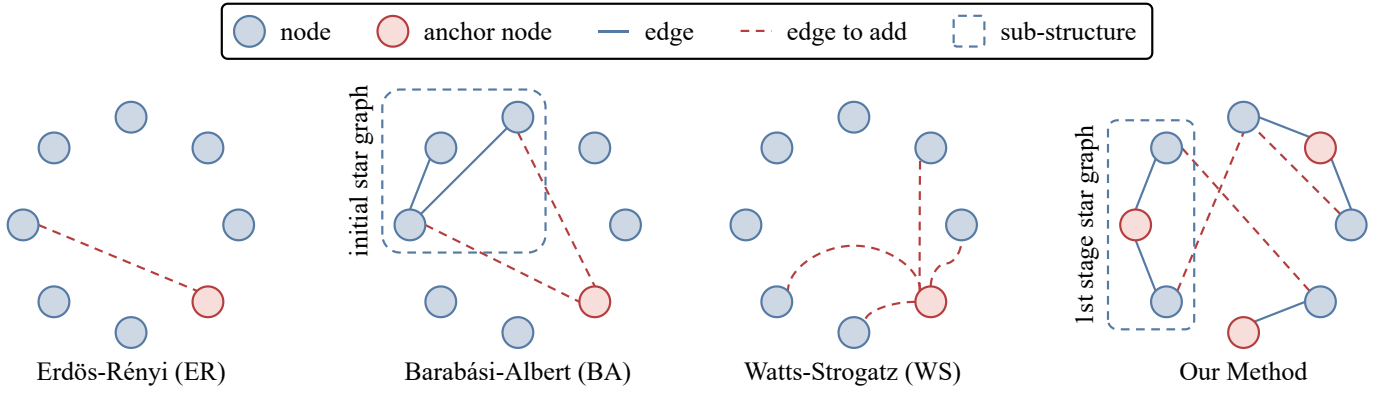


Fig. 2. Generation strategy comparison between several baselines and our method.

Given a set of graphs  $\mathbb{G} = \{\mathcal{G}_1, \dots, \mathcal{G}_{|\mathbb{G}|}\}$  sampled from a particular scenario  $\mathcal{S}$ , each graph is under the distribution determined by the characteristics of  $\mathcal{S}$ , where  $\mathcal{G} \sim p_{\mathcal{S}}(\mathcal{G})$ . Graph generation is essentially a task of sampling from the given distribution  $p_{\mathcal{S}}$ . However, unfortunately,  $p_{\mathcal{S}}$  is not always known. Sometimes, even  $\mathbb{G}$  is unknown due to security concerns or unaffordable costs. In this case, we can only obtain basic graph information like the number of nodes and edges and generate random graphs via the universal observation  $p_{\mathcal{O}}$ . Our method builds on existing observations as follows:

*Observation 1:* For real-world systems, most of them show the heavy-tailed degree distribution [34]. In other words, the degree distribution of these graphs has the power-law or scale-free characteristics.

The scale-free property of graphs is not a new concept, and researchers have studied it extensively [45]. A general conclusion states that the degree distribution of random graphs is close to the Poisson distribution, which is

$$P(X = d) = e^{-\lambda} \frac{\lambda^d}{d!}, \quad (1)$$

where  $d$  and  $\lambda$  are the selection and expectation of the node degree, respectively. We use  $P(k_0|\lambda_0)$  as a shorthand for  $P(X = k_0)$  with  $\lambda = \lambda_0$ .

At this point, we can give a complete definition of the problem concerned in this paper.

*Definition 2 (Problem Statement):* Given a set of graphs  $\mathbb{G}$ , we aim to create a generated set  $\hat{\mathbb{G}}$  from the restricted information (e.g.,  $N$ ,  $M$ ) under the premise that the ground truth distribution  $p_{\mathcal{S}}$  is unknown. Since  $p_{\mathcal{S}}$  is limited, the goal is to leverage some universal observations  $p_{\mathcal{O}}$  (e.g., Observation 1) to make  $\hat{\mathbb{G}}$  closer to  $\mathbb{G}$ .

Table I presents some significant notations and their definitions involved in this paper.

## IV. METHODOLOGY

### A. Overview

Figure 2 shows an overview of our method, comparing the generation strategy with several baselines. Our method

generates graphs and updates the node selection probabilities hierarchically. In the first stage, we parse the original nodes based on the Poisson distribution to build initial star graphs led by anchor nodes (Sec. IV-B). In the second stage, we prioritize ensuring the connectivity between previous subgraphs. Next, we design the node selection strategy to generate the remaining edges through a degree mixing distribution (Sec. IV-C). The article followed is structured in order of the graph generation. We discuss the time complexity and limitations at the end of this section.

### B. First Step of Generation

Generating a graph  $\mathcal{G}$  directly from  $N$  and  $M$  is equivalent to randomly sampling from the search space of  $\binom{N}{M}$ , which is a bit low probability. Inspired by the recursive [36], [47], [48] and multi-level [37], [38] generation methods, we design our work in a hierarchical stepwise scheme to improve the rationality of the distribution of the graph generated. In the first generation step, we extend the initial graph like [45] into multiple substructures, defined as follows.

*Definition 3 (Substructure):* A substructure  $\mathcal{G}_{sub}^{(i)}$  is a smaller graph derived from the original graph  $\mathcal{G}$ , where  $\mathcal{V}_{sub}^{(i)} \subseteq \mathcal{V}$  and is set of nodes.  $(N_{sub}^{(i)} + 1, N_{sub}^{(i)})$  is a star graph that exits a node  $v_0^{(i)}$  connected to all other nodes  $v_j^{(i)}$  ( $j = 1, \dots, N_{sub}^{(i)}$ ). We call  $v_0^{(i)}$  an anchor node of  $\mathcal{G}_{sub}^{(i)}$ .

Our method builds a parsing process from a given graph  $(N, M)$  to a substructure sequence  $\mathcal{G}_{sub} = \{\mathcal{G}_{sub}^{(0)}, \dots, \mathcal{G}_{sub}^{(l-1)}\}$ , where  $\mathcal{G}_{sub}^{(i)} = (d_i + 1, d_i)$ ,  $d_i$  is the node degree of  $v_0^{(i)}$ , and  $l$  is the number of substructures. We sample the degree sequence  $D = \{d_0, \dots, d_{l-1}\}$  of anchor nodes through Equation 1, guiding the generation of  $\mathcal{G}_{sub}$ , where  $D \sim P(\lambda)$ ,  $\sum_{i=0}^{l-1} d_i = N - l$ . Given  $(N, M)$ , we leverage the available information to estimate the average degree expectation, where  $\lambda = \frac{2M}{N} = \bar{D}$ . For example, Figure 2 presents a graph with eight nodes. In the first stage, we divide it into three substructures, where  $D = \{3, 3, 2\}$ .

When sampling  $D$ , it cannot avoid the appearance of exotic structures (e.g., star graphs), though the probability of large

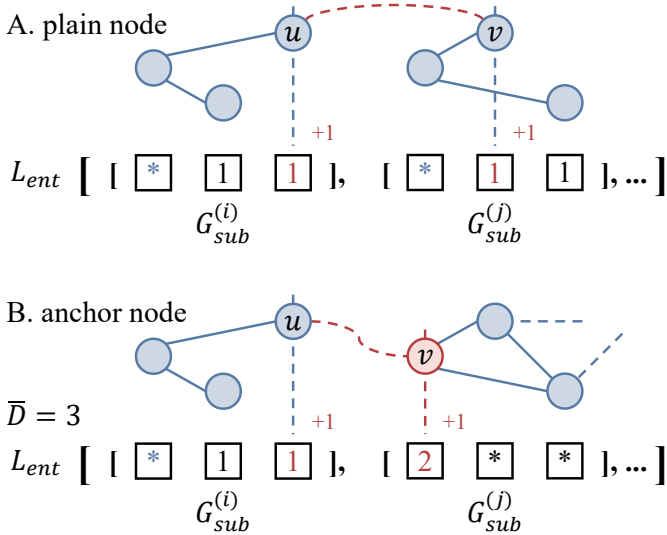


Fig. 3. Illustration of the edge generation. (A) connection to plain nodes. (B) connection to anchor nodes.

degrees is too low to zero. Therefore, we focus on two parameters to control the tolerance for unique structures when generating graphs. Similar to [45], [46], the first parameter we take into account is the max degree  $d_{max}$ . The 1-hop neighborhood of a center node shows wealthy local information, which builds the aggregation in the message-passing mechanism [39]. Inspired by this, we limit the number of edges elicited by each node with the  $d_{max}$  to fit the ground truth situation. And that is why we sample anchors first and build the star graph instead of any other structures. The second parameter is a truncation against Equation 1. For large degrees, denoted by  $d_\infty$ , it shows that

$$P(d_\infty|\bar{D}) \simeq 0 < P(0|\bar{D}), \quad (2)$$

where  $d_\infty \gg \bar{D}$ . Since a connected graph does not have nodes of degree 0, we can approximately remove  $d_\infty$  or more than  $d_\infty$  cases. We define  $k$  to be the smallest positive integer satisfying this equation. For example, Figure 2 gives a graph (8,8) with  $\bar{D} = 2$  and  $d_{max} = 3$ . In this case, we have  $P(0|2) \simeq 0.14$ ,  $P(3|2) \simeq 0.18$ . For a star graph (8,7) with equal nodes, the probability of the anchor node is  $P(7|\frac{2 \times 7}{8}) \simeq 0.0017$ , 100 times less than  $P(0|\frac{2 \times 7}{8})$ . We further design experiments to analyze the effect of combining two parameters on our method (Sec. V-D).

### C. Hierarchical Poisson Generation Strategy

After the first stage, we split the whole graph into a sequence of substructures, ensuring the generation of  $N$  nodes and carrying a small amount of edges. In the second stage, we generate the remaining edges gradually. Instead of [44] directly specifying the probability of edge generation, we build edges by selecting two endpoints. Inspired by [37], [47], we expand  $D$  into a list of entries  $L_{ent}$  as follows.

**Definition 4 (Entry):**  $L_{ent}$  is a list of entries, and  $L_{ent}[i]$  represents the degree sequence  $D_{sub}^{(i)}$  of  $\mathcal{G}_{sub}^{(i)}$ , where  $D_{sub}^{(i)}[0]$

### Algorithm 1 Build the Probability List

**Require:** the entry list  $L_{ent}$ ;

**Ensure:** the probability list  $plist$ , the indices list  $nlist$ ;

```

1:  $plist \leftarrow []$ ,  $nlist \leftarrow []$ ;
2: for  $i = 0, \dots, l - 1$  do
3:   compute  $s_{sub}^{(i)}$  according to Equation 4;
4:    $tlist \leftarrow []$ ;
5:   for  $j = 0, \dots, N_{sub}^{(i)}$  do
6:     compute  $Pr(v_j^{(i)})$  according to Equation 3;
7:     add index  $[i, j]$  to  $nlist$ ;
8:     add  $Pr(v_j^{(i)})$  to  $tlist$ ;
9:   end for
10:  add  $tlist$  to  $plist$ ;
11: end for
12: normalize  $plist$  under Equation 6;
13: return  $plist$ ,  $nlist$ 

```

is the degree of the  $v_0^{(i)}$ . We use  $L_{ent}[i][j]$  to refer to the node  $v_j^{(i)}$  located in  $\mathcal{G}_{sub}^{(i)}$ , forming an entry. For example, in Figure 3,  $L_{ent}[0][2]$  represents node  $u$ .

This auxiliary structure costs additional  $\mathcal{O}(N)$  space, assisting the probability list generation. We independently sample nodes  $u$  and  $v$  to form the edge  $e_{uv}$ . For each node  $v_j^{(i)}$ , the probability is as follows:

$$Pr(v_j^{(i)}) = s_{sub}^{(i)} \cdot P(L_{ent}[i][j] + 1|\bar{D}). \quad (3)$$

The probability consists of two parts:  $s_{sub}^{(i)}$  represents the probability of entering  $\mathcal{G}_{sub}^{(i)}$ , and  $P(L_{ent}[i][j] + 1|\bar{D})$  represents the sampling probability of the node jumping to the next degree of the current one based on Equation 1.  $s_{sub}^{(i)}$  refers to the preferential attachment theory proposed by [45].

**Theorem 1 (Preferential Attachment):** The more connections between nodes, the more likely it is to receive new connections. Consequently, there are central nodes or hubs in networks linking to abundant new nodes.

Since the first stage creates independent substructures, we naturally use  $N_{sub}^{(i)}$  to calculate the probability of connecting  $\mathcal{G}_{sub}^{(i)}$  with the formula:

$$s_{sub}^{(i)} = \frac{N_{sub}^{(i)}}{N}. \quad (4)$$

Each node located in  $\mathcal{G}_{sub}^{(i)}$  shares Equation 4 and adjusts itself according to the next-degree distribution of the current one, which is  $P(L_{ent}[i][j] + 1|\bar{D})$ . This design is a variant of [40] based on the desired degree theory.

**Theorem 2 (Desired Degree):** It can estimate the probability of selecting nodes via the occurrence of nodes with a particular degree  $d_*$ , called the desired degree.

Our method samples nodes according to the current  $L_{ent}$  and updates constantly. According to the assumptions in [37], [40], the process of selecting nodes  $u$  and  $v$  is independent. Thus, the probability of an edge is

$$P_{e_{uv}} = \bar{P}r(u) \cdot \bar{P}r(v), \quad (5)$$

**Algorithm 2** Our Method: Hierarchical Poisson Generation

**Require:** the number of nodes  $N$ , the number of edges  $M$ , the max degree  $d_{max}$ ;

**Ensure:** the generated graph  $\mathcal{G}$ ;

```

1:  $\bar{D} \leftarrow \frac{2M}{N}$ ,  $\mathcal{E} \leftarrow \emptyset$ ;
2:  $\mathcal{G}_{sub} \leftarrow [(d_{max} + 1, d_{max})]$ ,  $sN \leftarrow N - d_{max} - 1$ ;
3: while  $sN > 0$  do
4:   sample one possible  $d \sim P(\bar{D})$ ;
5:   add a star graph  $(d + 1, d)$  to  $\mathcal{G}_{sub}$ ;
6:    $sN \leftarrow sN - d - 1$ ;
7: end while
8: build a degree list  $L_{ent}$ ;
9: for all  $\mathcal{G}_{sub}^{(i)} \in \mathcal{G}_{sub}$  do
10:  sample a node  $u \in \mathcal{V}_{sub}^{(i)}$ ;
11:  build a probability list  $plist$ ;
12:  sample a node  $v \in \mathcal{V}_{sub}^{(j)}$ , ( $j \neq i$ ) based on  $plist$ ;
13:  add edge  $e_{uv}$  to  $\mathcal{E}$  and update  $L_{ent}$ ;
14: end for
15: build a graph  $\mathcal{G}$  based on  $\mathcal{G}_{sub}$  and  $\mathcal{E}$ ;
16:  $\mathcal{E} \leftarrow \emptyset$ ,  $\mathcal{E}' \leftarrow \emptyset$ ,  $sM \leftarrow M - |\mathcal{E}_{\mathcal{G}}|$ ;
17: while  $sM > 0$  do
18:  build a probability list  $plist$ ;
19:  sample a pair  $u, v$  based on  $plist$ ;
20:  add edge  $e_{uv}$  to  $\mathcal{E}$  and update  $L_{ent}$ ;
21:   $sM \leftarrow sM - |\mathcal{E}|$ ,  $\mathcal{E}' \leftarrow \mathcal{E}' \cup \mathcal{E}$ ,  $\mathcal{E} \leftarrow \emptyset$ ;
22: end while
23: add edges in  $\mathcal{E}'$  to  $\mathcal{G}$ ;
24: return  $\mathcal{G}$ 

```

where  $\bar{P}r(\cdot)$  is the probability after normalization, satisfying the probability sum of 1, that is

$$\sum_{i=0}^{l-1} \sum_{j=0}^{N_{sub}^{(i)}} \bar{P}r(v_j^{(i)}) = 1. \quad (6)$$

Algorithm 1 gives the procedure to build the probability list  $plist$  through  $L_{ent}$ . Since we sample anchor nodes based on the Poisson distribution, where  $D \sim P(\bar{D})$ , the expectation of the outer loop (line 2) is  $\mathbb{E}(l) = \frac{N}{\bar{D}+1}$ , and the inner (line 5) is  $\mathbb{E}(N_{sub}^{(i)}) = \bar{D} + 1$ . Thus, our method needs  $\mathcal{O}(N)$  to build the probability list each time.

In addition, our method prioritizes establishing connections between non-anchor nodes. Figure 3 illustrates the edge generation strategy under different node types. Given the max degree  $d_{max}$  constraint, we set  $Pr(v_0^{(i)}) = 0$  if existing non-anchor nodes whose degrees are less than  $d_{max}$ . We use \* to mask the corresponding positions  $L_{ent}[i][0]$ , as shown in Figure 3(A). After sampling the nodes  $u$  and  $v$ , the change of degree updates in  $L_{ent}$  from 1 to 2. As the number of edges increases, as shown in Figure 3(B), there will be a case where all non-anchor nodes have connected  $d_{max}$  edges like  $\mathcal{G}_{sub}^{(j)}$ . In this case, we mask the  $L_{ent}$  of the non-anchor nodes with \* and restore the anchor node to its current degree. For example, in Figure 3(B), we set  $L_{ent}[j][0] = 2$ . After sampling the node

pair, the update is the same as in 3(A). If the anchor node  $v_0^{(i)}$  exceeds  $d_{max}$ , too, we mask this  $\mathcal{G}_{sub}^{(i)}$  without visiting anymore.

Finally, we give the pseudocode of our method, as shown in Algorithm 2. Our method contains three parts. Firstly, we select anchor nodes and build the initial star graphs in the first stage (lines 2-7). Next, we ensure the previous graph connection at the beginning of the second stage (lines 9-14). And finally, we create the remaining edges (lines 17-22). Note that our method is hierarchical, and each part includes an update of the probability, which guarantees the accuracy of the generation.

**D. Theoretical Proof**

Our method partitions  $\mathcal{V}$  into two sets of nodes: a set  $\mathcal{V}_a$  of anchors and a set  $\mathcal{V}_{na}$  of non-anchors.  $D \sim P(\bar{D})$  initializes  $\mathcal{V}_a = \{v_0^{(0)}, \dots, v_0^{(l-1)}\}$ , thus  $\mathcal{V}_a \sim P(\bar{D})$ .  $\mathcal{V}_{na}$  calculates the sampling probability according to Equation 3, where we have

$$\begin{aligned} \mathbb{E}(\mathcal{V}_{na}) &= \sum_d d \cdot \bar{P}r(v_{na}; d) \\ &= \sum_d d \cdot \left[ \sum_i s_{sub}^{(i)} \cdot P(d|\bar{D}) \right] \\ &= \sum_d d \cdot \left[ P(d|\bar{D}) \cdot \sum_i s_{sub}^{(i)} \right] \\ &= \left[ \sum_d d \cdot P(d|\bar{D}) \right] \cdot \underbrace{\left[ \sum_i s_{sub}^{(i)} \right]}_1 \\ &= \mathbb{E}[d \sim P(\bar{D})] \cdot 1 = \bar{D}. \end{aligned} \quad (7)$$

In the actual generation process, there are a small number of nodes  $\mathcal{V}_e$  out of distribution due to the scaling of Equation 4 and the hierarchical sampling strategy in Figure 3. However, since  $|\mathcal{V}_e| \ll |\mathcal{V}|$ , our method maintains the conclusion in Observation 1.

We further discuss the expectation of Equation 3. Considering that anchor nodes guide the computation of Equation 4,  $s_{sub}^{(i)}$  is independent of the non-anchor node degree selection. So we have:

$$\begin{aligned} \mathbb{E} \left[ Pr(v_j^{(i)}) \right] &= \mathbb{E} \left[ s_{sub}^{(i)} \cdot P(L_{ent}[i][j] + 1|\bar{D}) \right] \\ &= \underbrace{\mathbb{E} \left[ s_{sub}^{(i)} \right]}_{Eq. 4} \cdot \mathbb{E} \left[ P(L_{ent}[i][j] + 1|\bar{D}) \right] \\ &= \frac{\mathbb{E} \left[ N_{sub}^{(i)} \right]}{N} \cdot \underbrace{P(\mathbb{E}(L_{ent}[i][j] + 1)|\bar{D})}_{Eq. 7} \\ &= \frac{\bar{D} + 1}{N} \cdot P(\bar{D}|\bar{D}) = \frac{e^{-\bar{D}}(\bar{D} + 1)\bar{D}^{\bar{D}}}{N\bar{D}}. \end{aligned} \quad (8)$$

It means that we no longer consider equivalently in node selection. Given the sparsity  $c$ , our method can maintain a probability expectation higher than  $\frac{1}{N}$  for a large number of nodes. For example, when  $c = 0.2358$ , Equation 8 exceeds the average selection if  $N \geq 20$ .

In addition, according to [44], we have the following theorem:

*Theorem 3 (Connectivity):* To ensure that the graph is connected, the number of edges should satisfy

$$M = \lfloor \frac{1}{2}N \log N + \epsilon N \rfloor, \quad (9)$$

where  $\lfloor x \rfloor$  is the integer part of  $x$  and  $\epsilon$  is an arbitrary fixed real number.

We can obtain three thresholds concerning the edge probability  $P_E$  of random graphs, proved by [41], [44]. The first is  $P_2 = \frac{\bar{D}}{N-1}$ , a plain selection for  $\bar{D}$  edges drawing from a center node. The second is  $P_3 = \frac{\log N}{N-1}$ , showing fewer isolated nodes. The last is  $P_4 = \frac{2 \log N}{N-1}$ , ensuring no isolated nodes exist. This series of probabilities is essentially a consideration of the sparsity of the graph, where the expected number of edges is  $M = \frac{N(N-1)}{2} \cdot P_E$ , drawing that  $c = P_E$ . Taking  $P_4$  as an example, our method picks one node with a higher probability than the average selection when  $N \geq 142$ .

### E. Time Complexity

The time complexity of our proposed method contains three parts. The first part is the parse phase. Given a graph  $(N, M)$ , our method generates initial star graphs under the Poisson distribution of  $\mathcal{P}(\lambda)$ , with  $\mathcal{O}(\frac{N}{\lambda} \cdot \log N)$  time complexity. The second part connects sub-structures, scanning each supernode once. For possible edge connecting  $\mathcal{G}_{sub}^{(1)}$  and  $\mathcal{G}_{sub}^{(2)}$  picked, our method decides which entries  $u$  and  $v$  the edge belongs to, where  $u \in \mathcal{V}_{sub}^{(1)}, v \in \mathcal{V}_{sub}^{(2)}$ , which costs a quadratic computation  $\mathcal{O}(\frac{N}{\lambda} \cdot N)$  to build the probability matrix for each scanning. The third part is to rebuild the rest of the  $M - N$  edges, which costs  $\mathcal{O}(\mathcal{K}N + \sum_{\mathcal{K}} \bar{M} \log N)$  in total, where  $\mathcal{K}$  is the number of scans and  $\bar{M}$  is the average edges picked each time. Our method generates average  $\frac{M}{\mathcal{K}}$  edges and updates the probability matrix like the second part. We could estimate  $\mathcal{K} \simeq \log M$  in a logarithmic descent speed. Thus, the time complexity of the third part is  $\mathcal{O}(N \log M + M \log N)$ . The final time complexity is the sum of all three parts above. To guarantee the graph connectivity, we approximate  $M$  with the probability of  $P_E = \frac{\log N}{N-1}$ , where  $M = \frac{N(N-1)}{2} \times P_E = \frac{N \log N}{2}$ . Since  $\lambda = \bar{D}$ , the time complexity above is equal to  $\mathcal{O}[N + \frac{N^2}{\log N} + N \log(\frac{N \log N}{2}) + \frac{N \log^2 N}{2}]$ .

In practice, however, edges are far more than nodes, where  $M = c \times \frac{N(N-1)}{2}, c \in (0, 1]$ . It shows that  $M \propto N^2$  rather than  $N \log N$ . So the complexity turns to  $\mathcal{O}(\log N + N + N \log N + N^2 \log N)$ , which eventually bounds to  $\mathcal{O}(N^2 \log N)$  (constants omitted). It is slower than the plain method of comparing all node pairs. An extra generation step with  $\mathcal{O}(\log N)$  happens for every possible edge. We also design a  $\mathcal{O}(N^2)$  version degrading the frequency of updating the probability matrix. We will discuss this issue later in the experiments (Sec. V-G).

### F. Limitation

Since our method relies on Observation 1, our performance degrades for partial graphs without the scale-free property.

TABLE II  
ADVANCED DETAILS OF ALL 12 DATASETS.

Dataset	Category	deg.	clus.	orbit	sparse
ENZYMES	bioinformatics	3.86	0.45	3.92	0.16
MUTAG	molecule	2.19	0.00	1.14	0.14
NCII	molecule	2.16	0.00	1.11	0.09
PROTEINS	bioinformatics	3.78	0.51	3.29	0.21
deezer_ego_nets	social	4.29	0.51	54.9	0.23
IMDB-BINARY	social	8.89	0.95	40.3	0.52
IMDB-MULTI	social	8.10	0.97	27.2	0.77
REDDIT-BINARY	social	2.34	0.05	4.2k	0.02
CLUS	synthetic	5.91	0.66	18.4	0.42
EGO	synthetic	1.99	0.00	6.32	0.01
GRID	synthetic	3.11	0.00	3.11	0.12
TREE	synthetic	1.86	0.00	0.83	0.14

Experimental results further illustrate this limitation (Sec. V-B). The closer the ground truth distribution is to a strict power law, the better our generation is.

## V. EXPERIMENTS

### A. Experimental Settings

1) *Datasets:* We perform experiments on eight real-world and four synthetic datasets to thoroughly evaluate our work. Datasets are from three categories: bioinformatics & molecule (a-d), social networks (e-h), and synthetic (i-l). Descriptions are listed below. **(a) ENZYMES** is derived from the BRENDA enzyme database, which shows the protein tertiary structures. It contains 600 graphs from 6 enzyme classes, each having average nodes and edges of 32.6 and 62.1. **(b) MUTAG** represents chemical compounds, having 188 samples to predict their mutagenicity on Salmonella typhimurium. It is a smaller dataset with average nodes and edges of 17.9 and 19.8. **(c) NCII** is a dataset of chemical compounds the same as the MUTAG. Among 4,110 graphs, each has an average of 29.9 nodes and 32.3 edges, categorized by positive or negative against cell lung cancer. **(d) PROTEINS** is a dataset of proteins classified by whether they are enzymes or not. There are 1,113 graphs with an average of 39.1 nodes and 72.8 edges.

**(e) deezer\_ego\_nets** is a user friendship network from the music service Deezer. It has 9,629 graphs, each having an average of 23.5 nodes and 65.3 edges. **(f) IMDB-BINARY** shows a movie collaboration of 1,000 actors/actresses in IMDB. These graphs come from two categories: Action and Romance. Each graph has 19.8 nodes and 96.5 edges. **(g) IMDB-MULTI** is the same as its BINARY version, except for the multi-class graphs. It has 1,500 graphs, with average nodes and edges of 13.0 and 65.9. **(h) REDDIT-BINARY** consists of 2,000 graphs of online discussions on Reddit, labeled by QA-based or discussion-based community. It is our largest dataset, each having 429.6 nodes and 497.8 edges on average.

All datasets above are real-world and from TUDataset [42]. Next are four synthetic datasets drawing various characteristics, each containing 200 graphs. **(i) CLUS** is the graph from the Holme and Kim algorithm [43], with power-law degree distribution and approximate average clustering. **(j) EGO** generates ego networks from power law degree sequences with average nodes of 150. **(k) GRID** is standard 2D grid

TABLE III  
MMD EVALUATION BETWEEN BASELINES AND OUR METHOD.

Methods	ENZYMES			MUTAG			NCII			PROTEINS		
	deg.	clus.	orbit	deg.	clus.	orbit	deg.	clus.	orbit	deg.	clus.	orbit
ER	0.2488	0.6522	0.3775	0.1688	0.2501	0.0119	0.2125	0.2014	0.0242	0.2927	0.5814	0.4779
BA	0.8302	<b>0.3198</b>	0.7207	1.0271	1.3066	0.6054	1.0987	1.1966	0.9007	0.9123	<b>0.2132</b>	0.7784
WS	0.6769	0.9314	<b>0.0657</b>	0.0821	<b>0.0233</b>	0.0095	0.1553	0.0278	0.0063	0.8293	0.9109	<b>0.1064</b>
MMSB	1.6808	1.3862	0.3420	0.9803	1.3099	0.0539	0.8707	0.2793	0.0434	1.6263	1.3005	0.2668
Kronecker	1.4012	1.3862	0.6402	1.7907	1.8785	0.0603	1.6345	1.6594	0.0414	1.0575	1.3005	0.2460
Ours	<b>0.1659</b>	0.6304	0.3203	<b>0.0003</b>	0.0419	<b>0.0004</b>	<b>0.0087</b>	<b>0.0170</b>	<b>0.0001</b>	<b>0.2702</b>	0.5670	0.1838
Methods	deezer_ego_nets			IMDB-BINARY			IMDB-MULTI			REDDIT-BINARY		
	deg.	clus.	orbit	deg.	clus.	orbit	deg.	clus.	orbit	deg.	clus.	orbit
ER	0.2865	0.6186	0.3814	0.0812	0.7398	0.1525	0.0317	0.4710	0.0663	1.0232	0.0908	1.0088
BA	0.2543	0.3494	0.2149	0.1614	0.9386	0.1583	0.2825	1.0538	0.2122	1.6028	<b>0.0279</b>	0.2784
WS	0.4242	0.7007	0.5348	0.2443	0.8787	0.4040	0.0761	0.4913	0.1314	1.3336	0.1307	1.1000
MMSB	0.7714	1.2728	1.0237	0.3857	0.7217	0.4481	0.3850	0.6088	0.1742	-	-	-
Kronecker	0.4082	1.2285	0.4832	1.1343	1.8764	0.7516	1.7928	1.9521	0.6108	1.7002	0.1310	1.2000
Ours	<b>0.0463</b>	<b>0.1004</b>	<b>0.0045</b>	<b>0.0456</b>	<b>0.7215</b>	<b>0.1314</b>	<b>0.0180</b>	<b>0.4639</b>	<b>0.0502</b>	<b>0.4123</b>	1.1913	<b>0.1996</b>
Methods	CLUS			EGO			GRID			TREE		
	deg.	clus.	orbit	deg.	clus.	orbit	deg.	clus.	orbit	deg.	clus.	orbit
ER	0.1557	0.3700	0.1564	0.1425	0.2875	0.0147	0.3799	0.5371	0.0792	0.0841	0.2227	0.0020
BA	0.0880	0.2100	0.0606	0.0413	0.0000	0.0087	1.1267	1.4074	0.7096	0.2013	0.0000	0.0586
WS	0.3510	0.6344	0.2894	-	-	-	1.0814	<b>0.0470</b>	0.3745	-	-	-
MMSB	0.8183	1.0930	0.5017	-	-	-	1.6535	1.6784	0.3293	0.5927	0.0000	0.0217
Kronecker	0.9960	1.3256	0.7888	1.4997	0.0000	0.4574	1.9735	1.7947	0.4274	1.0424	0.0000	0.0246
Ours	<b>0.0821</b>	<b>0.1243</b>	<b>0.0600</b>	<b>0.0347</b>	<b>0.0000</b>	<b>0.0013</b>	<b>0.0481</b>	0.3218	<b>0.0093</b>	<b>0.0155</b>	<b>0.0000</b>	<b>0.0007</b>

TABLE IV  
MMD EVALUATION BETWEEN DEEP LEARNING SOTAs AND OUR METHOD.

Methods	ENZYMES			MUTAG			NCII			PROTEINS		
	deg.	clus.	orbit	deg.	clus.	orbit	deg.	clus.	orbit	deg.	clus.	orbit
GraphRNN MLP	1.6851	1.0127	1.0231	1.6539	1.9100	1.2918	1.7020	1.9439	1.1536	1.6673	1.0854	0.8910
+training	0.2042	1.2339	<b>0.1088</b>	0.2138	0.7723	0.0456	0.3920	0.6467	0.0825	0.2860	0.6573	0.3239
GraphARM	1.8721	1.7257	0.4734	1.7245	0.0000	0.0549	1.7009	0.0371	0.0470	1.9206	1.3667	0.2019
+training	1.7830	1.3862	0.2326	1.6387	<b>0.0000</b>	0.0532	1.6999	<b>0.0000</b>	0.0464	1.7909	1.3593	0.3079
GraphILE	0.7302	1.2613	0.7600	0.5061	1.2001	1.0278	0.6607	1.2002	1.1948	0.6023	0.5941	0.4550
+training	0.2333	<b>0.2603</b>	0.1121	0.5833	1.0054	0.9027	0.0446	0.7988	0.1271	0.2730	0.5773	0.1888
Ours	<b>0.1659</b>	0.6304	0.3203	<b>0.0003</b>	0.0419	<b>0.0004</b>	<b>0.0087</b>	0.0170	<b>0.0001</b>	<b>0.2702</b>	<b>0.5670</b>	<b>0.1838</b>
Methods	deezer_ego_nets			IMDB-BINARY			IMDB-MULTI			REDDIT-BINARY		
	deg.	clus.	orbit	deg.	clus.	orbit	deg.	clus.	orbit	deg.	clus.	orbit
GraphRNN MLP	1.2262	1.3054	0.5834	1.0155	1.8265	0.4083	1.2608	1.7468	1.1993	1.8544	0.7590	0.9275
+training	1.1688	1.3245	1.1597	0.5036	1.8412	0.7765	0.6925	1.5325	0.8245	0.6891	<b>0.1295</b>	1.1999
GraphARM	1.3041	1.2882	1.0891	1.3703	1.8764	1.3149	0.7155	0.8996	-	-	-	-
+training	0.8506	0.9830	1.2827	1.1919	1.3964	1.2144	0.9056	<b>0.0304</b>	-	-	-	-
GraphILE	0.6224	1.1985	1.2144	0.6126	1.3221	1.2408	0.3850	1.0126	0.4014	-	-	-
+training	0.2295	0.4003	0.5025	0.5981	1.3465	0.4415	0.3742	0.8134	0.3998	-	-	-
Ours	<b>0.0463</b>	<b>0.1004</b>	<b>0.0045</b>	<b>0.0456</b>	<b>0.7215</b>	<b>0.1314</b>	<b>0.0180</b>	0.4639	<b>0.0502</b>	<b>0.4123</b>	1.1913	<b>0.1996</b>
Methods	CLUS			EGO			GRID			TREE		
	deg.	clus.	orbit	deg.	clus.	orbit	deg.	clus.	orbit	deg.	clus.	orbit
GraphRNN MLP	0.2489	0.7418	0.8339	1.8982	1.6031	1.0489	1.8623	1.9928	1.0156	1.4897	1.9996	1.1506
+training	0.5203	0.7172	0.6988	0.9116	0.4883	0.4290	0.8239	0.1763	1.1837	0.7043	0.0892	0.3258
GraphARM	1.3535	1.4196	1.1840	1.4053	0.0000	0.0303	1.9733	0.0000	0.4525	1.5013	0.0000	0.0233
+training	1.3362	1.4200	0.7786	1.4160	<b>0.0000</b>	0.0286	1.9460	<b>0.0000</b>	0.3720	1.4871	<b>0.0000</b>	0.0216
GraphILE	0.1293	0.4000	0.4538	0.6892	0.0000	0.5790	0.6400	1.2003	1.2129	0.6348	1.2000	0.0243
+training	0.2118	0.9729	0.2886	0.6708	0.0000	0.5540	0.4095	2.0000	1.0415	0.5789	1.0051	0.9097
Ours	<b>0.0821</b>	<b>0.1243</b>	<b>0.0600</b>	<b>0.0347</b>	0.0000	<b>0.0013</b>	<b>0.0481</b>	0.3218	<b>0.0093</b>	<b>0.0155</b>	0.0000	<b>0.0007</b>

graph from 10x10 to 20x20. (I) **TREE** generates a tree with 100 to 200 nodes converted from a uniformly random Prüfer sequence.

Furthermore, Table II shows four more advanced details: average degree, clustering coefficient, orbit count, and sparsity.

2) *Baselines*: We compare five traditional baselines: Erdős-Rényi (ER) [44], Barabási-Albert (BA) [45], Watts-Strogatz (WS) [46], Mixed-Membership Stochastic Block

(MMSB) [47], and Kronecker [48]. We also pick several popular and recent models: GraphRNN [49], GraphARM [50], and GraphILE [51].

3) *Evaluation Metrics*: We use the Maximum Mean Discrepancy (MMD) [52] to evaluate the quality of generated graphs. Following [49], we compute MMD scores for the average degree, clustering coefficient, and orbit count.



TABLE V  
ABLATION OF TWO PARAMETERS ON ALL THREE DATASET CATEGORIES.

$d_{max}$	$k$	Bioinformatics & Molecules			Social Networks			Synthetic		
		deg.	clus.	orbit	deg.	clus.	orbit	deg.	clus.	orbit
✓	×	<b>0.1113</b>	<b>0.3141</b>	<b>0.1261</b>	<b>0.0318</b>	0.5927	<b>0.0908</b>	<b>0.0451</b>	<b>0.1115</b>	<b>0.0178</b>
×	×	0.2173	<u>0.5560</u>	0.2098	0.4656	0.7083	0.3385	0.2166	<u>0.2026</u>	0.1814
✓	✓	<u>0.1654</u>	0.6144	0.2190	<u>0.1390</u>	<b>0.4909</b>	<u>0.1686</u>	<u>0.1369</u>	0.2344	<u>0.0549</u>
×	✓	0.2124	0.6557	0.2112	0.5921	<u>0.5474</u>	0.6100	0.3519	0.3876	0.3415

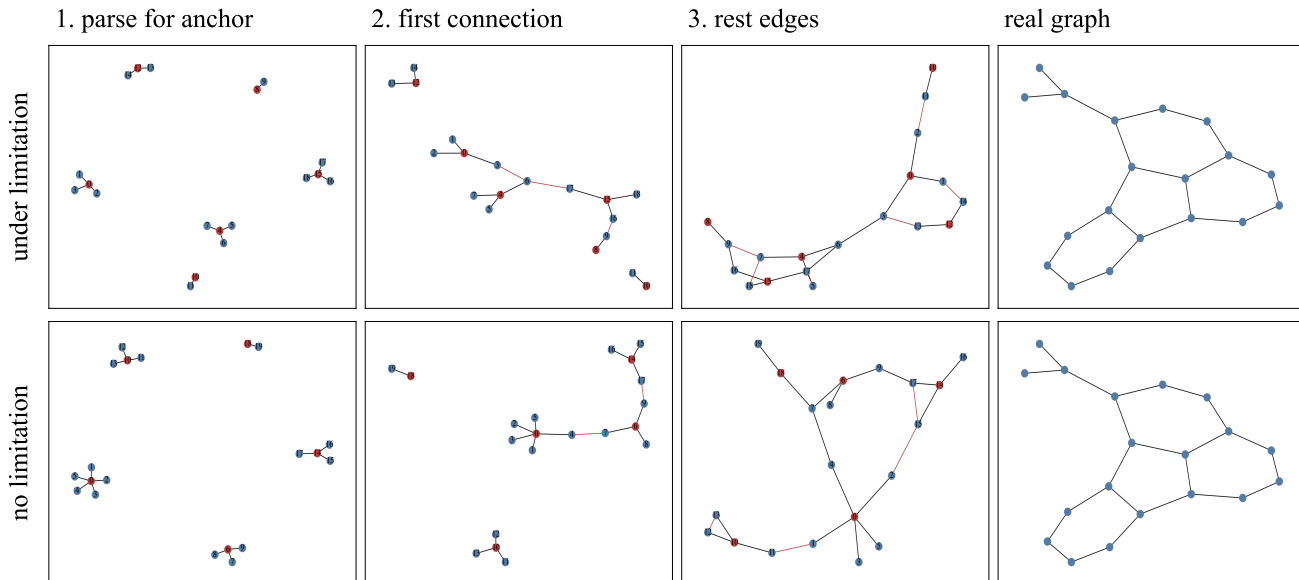


Fig. 4. Generation steps with/without  $d_{max}$  limitation. Anchor nodes and edges to add in each step are in red.

4) *Implementation Details*: We use the same sources as [49] to conduct four traditional methods, while WS is from the open toolkit NetworkX [53]. As for deep learning SOTAs, we try our best to reproduce them based on their open-source codes. All experiments are trained and evaluated on an NVIDIA RTX 3050 OEM 24GB GPU and 32GB memory.

## B. Main Results

Table III shows the comparison results of our method to baselines on all 12 datasets. The best and second scores are in **bold** and underlined, respectively. Absences in the table, marked by -, denote the failure of generation (e.g., self-loop, no edges, etc.) or out of time (OOT). Generally, our method achieves better generation results than traditional works and deep learning SOTAs. Although some scores of particular datasets are not the best, we are still in the top two performances, and taking all metrics together, we can provide significant improvement. For example, for the average degree, our method can reach an accuracy of  $10^{-4}$ , while the competitive model, WS, can only at  $10^{-2}$  in MUTAG.

Among all datasets, only the average clustering coefficient of REDDIT-BINARY fails to achieve a satisfactory result. The same occurs for some other datasets. Such a phenomenon reveals the limitation of our method, whose scale-free property introduced by Poisson distribution may not fit the complicated case of real-world scenarios (e.g., high clustering). But, in gen-

eral, our method can adapt to the vast majority of cases when data is limited, especially when the distribution is unknown. We will discuss it later with various alternate distributions to show the superiority of our method.

## C. Comparison with Deep Generative Models

Although deep generative models critically suffer when no training data is available, we are still interested in their performance. Table IV shows the results. For each baseline, we first evaluate all datasets with only the initialization state, which simulates the situation of no training data. Next, we train all models with a fixed number of steps, assuming there are limited numbers for fetching training data. Results show that the limitation of training data has disastrous effects on deep learning models. On the one hand, models cannot work competently without training. On the other hand, the undertrained model does not have enough time to learn implicit characteristics in the dataset, leading to the instability of early results. In most cases, models fail to optimize the results of all three matrices simultaneously. However, the training always works. Models outperform our method after limited training steps under partial datasets. For example, GraphRNN has *deg.* and *orbit* scores of 0.20 and 0.11 after 100 training epochs, which shows a 0.2 increase in *orbit* with only a 0.04 decrease in *deg.* To sum up, our method retains its advantage when training is impossible. In the case of limited training, our

TABLE VI  
MMD EVALUATION UNDER VARIOUS DISTRIBUTIONS.

Methods	ENZYMES			MUTAG			NCI1			PROTEINS		
	deg.	clus.	orbit	deg.	clus.	orbit	deg.	clus.	orbit	deg.	clus.	orbit
Uniform	0.5415	<u>1.1109</u>	0.7837	0.3120	0.2950	0.0881	0.5154	0.2349	0.4064	0.4564	<u>0.6074</u>	0.2959
Normal	0.7961	1.1460	0.5190	<u>0.0223</u>	0.2209	0.0033	<u>0.0101</u>	0.0488	<u>0.0008</u>	0.6234	0.7956	<u>0.1865</u>
Exponential	1.6231	1.3789	0.4435	0.0857	0.2074	0.0092	0.3715	0.0279	0.0525	1.2945	1.2377	0.2489
Gamma	1.7603	1.7257	<u>0.4089</u>	0.3937	<u>0.0724</u>	0.0332	0.5470	<u>0.0181</u>	0.0345	0.8069	0.6879	0.1976
Pareto	<u>0.2177</u>	1.2123	0.4639	0.0672	0.3065	<u>0.0029</u>	0.1354	0.0469	0.0200	<u>0.4554</u>	0.7306	0.1998
Ours	<b>0.1659</b>	<b>0.6304</b>	<b>0.3203</b>	<b>0.0003</b>	<b>0.0419</b>	<b>0.0004</b>	<b>0.0087</b>	<b>0.0170</b>	<b>0.0001</b>	<b>0.2702</b>	<b>0.5670</b>	<b>0.1838</b>

Methods	deezer_ego_nets			IMDB-BINARY			IMDB-MULTI			REDDIT-BINARY		
	deg.	clus.	orbit	deg.	clus.	orbit	deg.	clus.	orbit	deg.	clus.	orbit
Uniform	<u>0.1098</u>	0.2198	0.0714	<u>0.1331</u>	0.7598	0.2249	0.1064	0.5144	0.1079	0.4488	<u>0.2060</u>	<u>0.2157</u>
Normal	0.1361	<u>0.2774</u>	0.0681	0.1516	<u>0.7259</u>	0.2165	0.0720	0.4963	0.1080	0.4360	1.2023	0.3767
Exponential	0.6029	1.3469	0.3978	1.1977	1.8764	0.5922	0.2722	0.6856	0.2023	0.4651	1.1388	0.3364
Gamma	0.4820	1.0957	0.1444	0.3357	0.7464	0.2286	0.2254	0.4888	0.1081	0.6313	<b>0.1307</b>	0.3999
Pareto	0.3154	0.5379	0.2428	0.3898	1.5852	0.5664	<u>0.0271</u>	0.5155	<u>0.1059</u>	<u>0.4126</u>	0.8336	0.3726
Ours	<b>0.0463</b>	<b>0.1004</b>	<b>0.0045</b>	<b>0.0456</b>	<b>0.7215</b>	<b>0.1314</b>	<b>0.0180</b>	<b>0.4639</b>	<b>0.0502</b>	<b>0.4123</b>	1.1913	<b>0.1996</b>

Methods	CLUS			EGO			GRID			TREE		
	deg.	clus.	orbit	deg.	clus.	orbit	deg.	clus.	orbit	deg.	clus.	orbit
Uniform	0.2368	0.4216	0.2680	0.8342	0.0000	0.5916	0.5937	0.7615	0.2094	0.1314	0.0059	0.0728
Normal	<u>0.1743</u>	<u>0.1842</u>	0.2039	0.2515	0.0000	0.0419	0.3614	0.5705	0.0243	0.0557	0.0000	<u>0.0009</u>
Exponential	0.9475	1.1553	0.2989	<u>0.1353</u>	0.0000	<u>0.0336</u>	0.4194	0.7172	0.0493	1.0230	0.0000	0.0016
Gamma	0.6039	0.8757	0.4299	0.6639	0.0000	0.1279	1.2909	1.2563	0.2825	0.4505	0.0000	0.0217
Pareto	0.2234	0.3474	<u>0.1539</u>	0.3088	0.0000	0.7013	<u>0.0645</u>	<u>0.5313</u>	<u>0.0105</u>	<u>0.0286</u>	0.0000	0.0072
Ours	<b>0.0821</b>	<b>0.1243</b>	<b>0.0600</b>	<b>0.0347</b>	<b>0.0000</b>	<b>0.0013</b>	<b>0.0481</b>	<b>0.3218</b>	<b>0.0093</b>	<b>0.0155</b>	<b>0.0000</b>	<b>0.0007</b>

TABLE VII  
PARAMETER SETTINGS.

Methods	$f(x)$	Default Settings
Uniform	$1/(b-a)$	equal probability
Normal	$e^{-(x-\mu)^2/2\sigma^2}/\sqrt{2\pi}\sigma$	$\mu = \bar{D}, \sigma = 1$
Exponential	$\lambda e^{-\lambda x}$	$\lambda = \bar{D}$
Gamma	$\beta^\alpha x^{\alpha-1} e^{-\beta x} / \Gamma(\alpha)$	$\alpha = \bar{D}, \beta = P_E$
Pareto	$kx^k_{min}/x^{k+1}$	$k = \bar{D}, x_{min} = d_{min}$
Ours	$\lambda^x e^{-\lambda}/x!$	$\lambda = \bar{D}$

TABLE VIII  
TIME EVALUATION BETWEEN BASELINES AND OUR METHOD.

Methods	IMDB-MULTI (sparse: 0.77)			Time (s)
	deg.	clus.	orbit	
ER	0.0317	0.4710	0.0663	<b>4.20E-5</b>
BA	0.2825	1.0538	0.2122	1.10E-4
WS	0.0761	0.4913	0.1314	2.30E-4
MMSB	0.3850	0.6088	0.1742	1.76E-4
Kronecker	1.7928	1.9521	0.6108	1.10E-3
Ours	0.0180	0.4639	0.0502	3.04E-4
Ours (Fast)	0.4462	0.5657	0.2134	<u>5.00E-5</u>

method can achieve stable and appreciable results under a fixed training step.

#### D. Parameter Studies

There are two parameters in our method: one is  $d_{max}$ , and the other is  $k$ . They both determine how tolerant the generation process is of particular graph cases. The former limits the maximum degree of each node and mainly affects the selection of anchor nodes. Figure 4 illustrates the comparison of generation steps with and without  $d_{max}$  limitation. For example, without  $d_{max} = 3$ , our method may generate  $\mathcal{G}_{sub} = (6, 5)$  in the first stage, which finally impacts the following edge selection. The star graph formed by the anchor node exceeding the  $d_{max}$

degree constraint will change the properties of the generated graph, creating structures out of distribution.

The latter is essentially a truncation. Since a connected graph has no node with 0 degrees, we can assume that nodes with a degree probability lower than  $P(0|\bar{D})$  do not exist. We define  $k$  to be the first positive integer satisfying  $P(k|\bar{D}) < P(0|\bar{D})$ , which controls whether small probability nodes occur. Table V shows the ablation experiments for the two parameters above, reporting the average MMD scores of the four datasets under each category. Results show that  $d_{max}$  contributes more to the performance than  $k$ , and a relatively conservative generation (strictly restricting the structures out of distribution) can also achieve good results.

#### E. Graph Generation under Various Distributions

We conduct a distribution ablation experiment to demonstrate the superiority of our method, replacing the Poisson distribution with other distributions. We pick five distributions: Uniform, Gaussian (standard normal), Exponential, Gamma, and Pareto. Table VII shows the detailed parameter settings. For a possible degree  $x = d$ , we consider the cumulative distribution function (CDF) as an approximation of its probability, where  $P\{x = d\} = P\{d-1 < x \leq d\}$ . Ablation results are in Table VI. Through experiments, we can draw some enlightened conclusions. Firstly, our method (Poisson distribution) achieves the best results, indicating that the observation of the scale-free property of which this paper is the basis is valid. Secondly, we observe from the underlined results that different prior distributions fit datasets in disparate categories. For example, Uniform and Normal are more suitable for social networks since dense graphs form high clustering, making edge selection of nodes in clusters tend to be consistent. Finally, Pareto is the closest to our

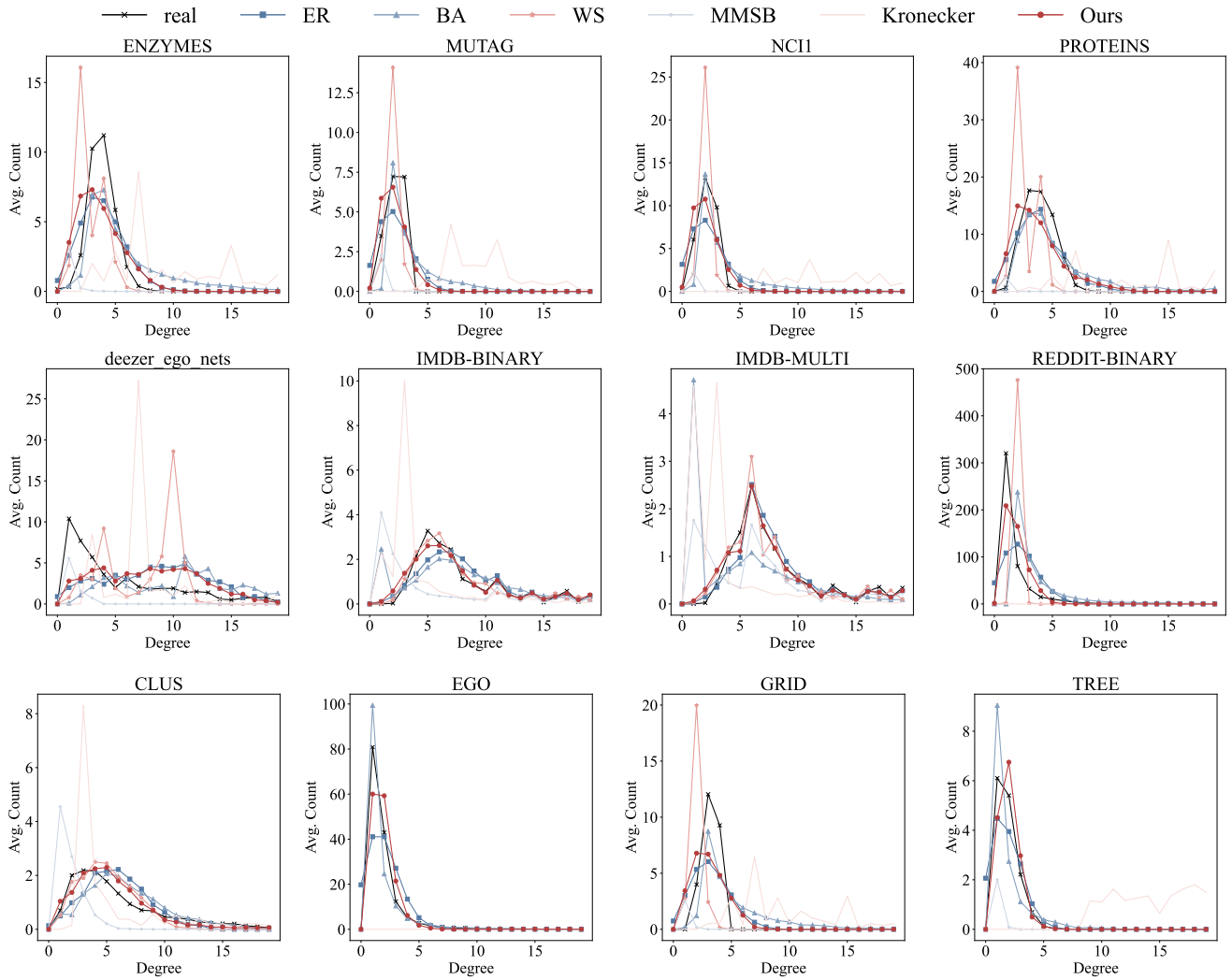


Fig. 5. Degree distribution comparisons between generated and real-world graphs.

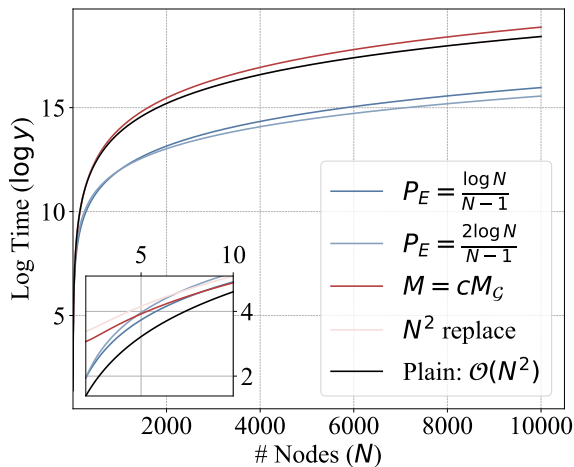


Fig. 6. Time analysis under different settings.

method among all the other distributions. Pareto is also a

distribution that illustrates the power law characteristics, but the results are still weaker than ours. In conclusion, although different datasets and distributions have their specific features, the Poisson distribution in our method is relatively one of the optimal choices in the scenario of unknown distribution.

#### F. Comparison with Real Degree Distributions

Until now, we have restricted access to the ground truth distribution. We are so curious about the difference between the degree distribution of the generated and real-world graphs in such a setting that we design experiments to collect those statistics. Figure 5 shows the results from baselines and our method. The x-axis represents the node degree with a truncation to count only the nodes with degrees less than 20, while the y-axis represents the average over all graphs in the datasets. Experimental results show that our method can generate graphs close to the ground truth distribution. Despite the differences between categories, we can see the scale-free characteristics of all datasets in Figure X. This property prevents the occurrence

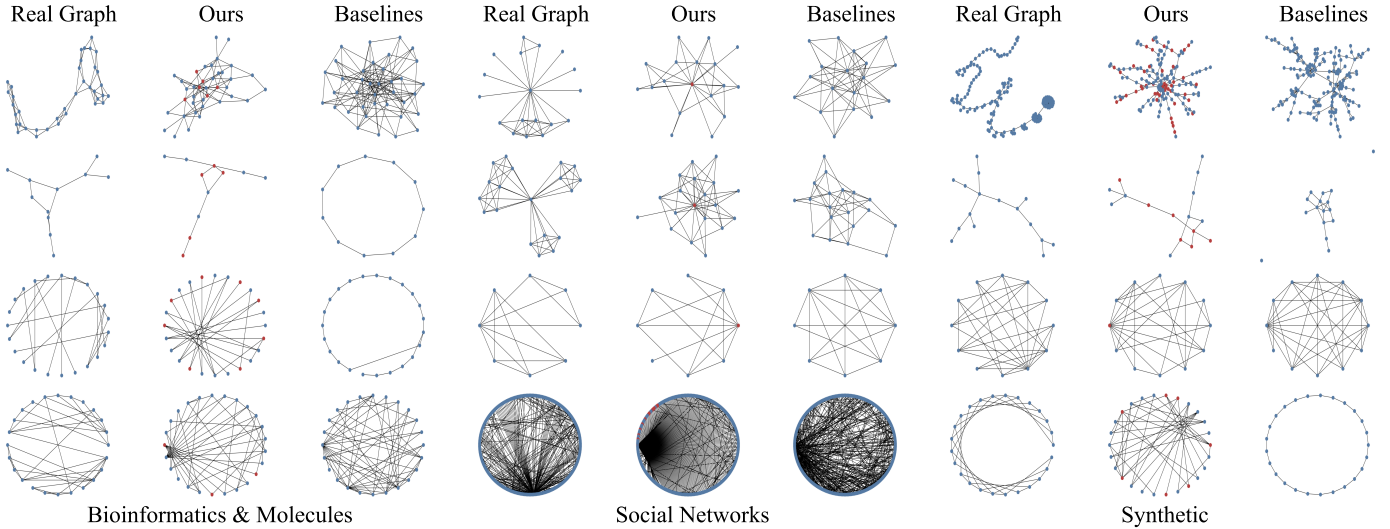


Fig. 7. Visualization of graphs of all categories. They are (from left to right, each consisting of three columns) bioinformatics & molecules, social networks, and synthetic graphs. Within each category, the first column is from the dataset, and the third is from baselines achieving competitive results. The second column is from our method, where anchor nodes are in red. We use various layouts for each row to represent different datasets.

of extra degrees when generating graphs. Another observation is that for cases with more complicated distributions, such as four social networks in the middle row, our method can also fit the fluctuation of the plots. For example, on IMDB-BINARY and IMDB-MULTI, our plots (red solid circle) almost coincide with the plots of ground truth (black cross). Some baselines may have a better coincidence in a particular degree interval than our method but severely fluctuate when dealing with all datasets along all degrees.

### G. Time Analysis

In this section, we further analyze the time cost of our method. Figure 6 shows the logarithmic time plot comparison under different settings. The x-axis represents the number of nodes in the graph, and the y-axis represents the corresponding runtime (in log form). As mentioned previously, the time consumption will ideally be two blue plots under the probability of  $P_E \in [\frac{\log N}{N-1}, \frac{2\log N}{N-1}]$ , which is lower than the plain algorithm of pairwise selection between nodes. In practice, however, edges are closer to being estimated in the manner  $M = cM_G$ , where  $c \in [0, 1]$ ,  $M_G$  represents the number of edges in the fully connected graph. The actual runtime is the red plot in the figure, where  $c = 0.2358$ , the average of the sparsity of all 12 datasets.

To alleviate this problem and strike a balance between performance and efficiency, we also design a scheme for  $\mathcal{O}(N^2)$ . Specifically, we no longer update the selection probabilities gradually and rely on the initial values to calculate each node pair, which turns to  $\mathcal{O}(M) \times \mathcal{O}(1)$ . Table VIII shows the calculation results under IMDB-MULTI. IMDB-MULTI is the densest among all datasets, with 0.77 times as many edges as the fully connected graph. Our conventional method is in the  $10^{-4}$  level, an order of magnitude behind ER's  $10^{-5}$ , and

comparable to other methods like BA. The fast version has a similar time cost as ER but at the price of performance. It is more suitable for high-density data like IMDB-MULTI, and other datasets can draw similar conclusions. When the graph gradually becomes sparse, we choose the conventional version to achieve better generation performance.

### H. Graph Visualization

We visualize the graphs generated by baselines and our method. Figure 7 illustrates the results. Our method can maximally recover the unique structures that may appear under the real-world distribution, such as loops (row 2, column 2), cluster centers (row 1, column 5), chains (row 2, column 8), etc. Since the ground truth distribution is unknown, there are still limitations in fully generating structures rich in semantics, for example, benzene rings (loops containing six nodes) in bioinformatics, standard 2D grids, etc. Our method best succeeds data with similar scale-free properties, where closer proximity means more prior knowledge of the distribution. Meanwhile, we reduce the generation of invalid structures, such as plain graphs (row 2, column 3), etc.

## VI. CONCLUSION

In this paper, we design a hierarchical Poisson generator for universal graphs under limited resources. We consider the scale-free property of graphs as an invariant feature and propose a two-stage generation strategy. We split the original set of nodes into multiple substructures by sampling anchor nodes according to the Poisson distribution, ensuring scale-free distribution and local clustering property. We also design a degree mixing distribution to sample the remaining edges, cooperating with selected thresholds, which can adjust the algorithm tolerance to exotic structures. The experimental results on 12 datasets in three categories show that our method

can fit the ground truth distribution and generate higher-quality graphs than SOTAs.

## REFERENCES

- [1] C. Wang, B. Wang, B. Huang, S. Song, and Z. Li, "FastSGG: Efficient Social Graph Generation Using a Degree Distribution Generation Model," in *ICDE*, 2021.
- [2] S. Xiang, D. Cheng, J. Zhang, Z. Ma, X. Wang, and Y. Zhang, "Efficient Learning-based Community-Preserving Graph Generation," in *ICDE*, 2022.
- [3] L. Zhang, D. Zhou, H. Tong, J. Xu, Y. Zhu, and J. He, "FairGen: Towards Fair Graph Generation," in *ICDE*, 2024.
- [4] H. Huang, L. Sun, B. Du, and W. Lv, "Conditional Diffusion Based on Discrete Graph Structures for Molecular Graph Generation," in *AAAI*, 2023.
- [5] Y. Zhu, Z. Ouyang, B. Liao, J. Wu, Y. Wu, C. Hsieh, T. Hou, and J. Wu, "MolHF: A Hierarchical Normalizing Flow for Molecular Graph Generation," in *IJCAI*, 2023.
- [6] G. Wei, Y. Huang, C. Duan, Y. Song, and Y. Du, "Navigating Chemical Space with Latent Flows," in *NeurIPS*, 2024.
- [7] H. Huang, L. Sun, B. Du, Y. Fu, and W. Lv, "GraphGDP: Generative Diffusion Processes for Permutation Invariant Graph Generation," in *ICDM*, 2022.
- [8] N. Gruver, S. D. Stanton, N. C. Frey, T. G. J. Rudner, I. Hotzel, J. L. Vanasse, A. Rajpal, K. Cho, and A. G. Wilson, "Protein Design with Guided Discrete Diffusion," in *NeurIPS*, 2023.
- [9] Y. Du, M. Plainer, R. Brekelmanns, C. Duan, F. Noé, C. P. Gomes, A. A. Guzik, and K. Neklyudov, "Doob's Lagrangian: A Sample-Efficient Variational Approach to Transition Path Sampling," in *NeurIPS*, 2024.
- [10] X. Guo, Y. Du, and L. Zhao, "Deep Generative Models for Spatial Networks," in *KDD*, 2021.
- [11] C. Zhang, X. Lyu, and Z. Tang, "TGG: Transferable Graph Generation for Zero-shot and Few-shot Learning," in *MM*, 2019.
- [12] S. Zhang, T. Li, S. Hui, G. Li, Y. Liang, L. Yu, D. Jin, and Y. Li, "Deep Transfer Learning for City-scale Cellular Traffic Generation through Urban Knowledge Graph," in *KDD*, 2023.
- [13] J. Yang, X. Jiang, Y. Guo, L. T. Yang, and J. Yang, "Generalize to Fully Unseen Graphs: Learn Transferable Hyper-Relation Structures for Inductive Link Prediction," in *MM*, 2024.
- [14] Bernardino Romera-Paredes and Philip Torr, "An embarrassingly simple approach to zero-shot learning," in *ICML*, 2015.
- [15] T. G. Armstrong, V. Ponnekanti, D. Borthakur, and M. Callaghan, "LinkBench: A database benchmark based on the Facebook social graph," in *SIGMOD*, 2013.
- [16] A. K. Joshi, P. Hitzler, and G. Dong, "LinkGen: Multipurpose linked data generator," in *ISWC*, 2016.
- [17] G. Bagan, A. Bonifati, R. Ciucanu, G. Fletcher, A. Lemay, and N. Advokaat, "gMark: Schema-driven generation of graphs and queries," in *TKDE*, 2016.
- [18] R. Milo, S. S. Orr, S. Itzkovitz, N. Kashtan, D. Chklovskii, and U. Alon, "Network Motifs: Simple Building Blocks of Complex Networks," in *Science*, 2002.
- [19] B. Samanta, A. De, G. Jana, V. Gomez, P. K. Chattaraj, N. Ganguly, and M. G. Rodriguez, "NeVAE: A Deep Generative Model for Molecular Graphs," in *JMLR*, 2020.
- [20] Y. Du, Y. Wang, F. Alam, Y. Lu, X. Guo, L. Zhao, and A. Shehu, "Deep Latent-Variable Models for Controllable Molecule Generation," in *BIBM*, 2021.
- [21] Y. Du, X. Guo, A. Shehu, and L. Zhao, "Interpretable Molecular Graph Generation via Monotonic Constraints," in *SDM*, 2022.
- [22] Y. Liu, X. Ao, F. Feng, Y. Ma, K. Li, T. Chua, and Q. He, "FLOOD: A Flexible Invariant Learning Framework for Out-of-Distribution Generalization on Graphs," in *KDD*, 2023.
- [23] Y. Liu, L. Zou, and Z. Wei, "Building Graphs at Scale via Sequence of Edges: Model and Generation Algorithms (Extended Abstract)," in *ICDE*, 2022.
- [24] S. Zheng, C. Wang, C. Wu, Y. Lou, H. Feng, and X. Yang, "Temporal Graph Generation Featuring Time-Bound Communities," in *ICDE*, 2024.
- [25] Clement Vignac and Pascal Frossard, "Top-N: Equivariant Set and Graph Generation without Exchangeability," in *ICLR*, 2022.
- [26] B. Qiang, Y. Song, M. Xu, J. Gong, B. Gao, H. Zhou, W. Ma, and Y. Lan, "Coarse-to-Fine: a Hierarchical Diffusion Model for Molecule Generation in 3D," in *ICML*, 2023.
- [27] T. Jia, H. Li, C. Yang, T. Tao, and C. Shi, "Graph Invariant Learning with Subgraph Co-mixup for Out-of-Distribution Generalization," in *AAAI*, 2024.
- [28] Martin Simonovsky and Nikos Komodakis, "Graphvae: Towards generation of small graphs using variational autoencoders," in *ICANN*, 2018.
- [29] Nicola De Cao and Thomas Kipf, "MolGAN: An implicit generative model for small molecular graphs," in *ICML*, 2018.
- [30] Y. Luo, K. Yan, and S. Ji, "Graphdf: A discrete flow model for molecular graph generation," in *ICML*, 2021.
- [31] H. Cao, C. Tan, Z. Gao, G. Chen, P. A. Heng, and S. Z. Li, "A survey on generative diffusion model," *arXiv preprint arXiv:2209.02646*, 2022.
- [32] F. Eijkelboom, G. Bartosh, C. A. Naesseth, M. Welling, and J. van de Meent, "Variational Flow Matching for Graph Generation," in *NeurIPS*, 2024.
- [33] A. Bonifati, I. Holubová, A. P. Pérez, and S. Sakr, "Graph Generators: State of the Art and Open Challenges," in *CSUR*, 2020.
- [34] Xiaojie Guo and Liang Zhao, "A Systematic Survey on Deep Generative Models for Graph Generation," in *TPAMI*, 2022.
- [35] C. Liu, W. Fan, Y. Liu, J. Li, H. Li, H. Liu, J. Tang, and Q. Li, "Generative Diffusion Models on Graphs: Methods and Applications," in *IJCAI*, 2023.
- [36] D. Chakrabarti, Y. Zhan, and C. Faloutsos, "R-MAT: A recursive model for graph mining," in *ICDM*, 2004.
- [37] T. G. Kolda, A. Pinar, T. Plantenga, and C. Seshadhri, "A scalable generative graph model with community structure," in *SISC*, 2014.
- [38] S. Edunov, D. Logothetis, C. Wang, A. Ching, and M. Kabiljo, "Darwini: Generating realistic large-scale social graphs," in *arXiv preprint arXiv:1610.00664*, 2016.
- [39] T. N. Kipf and M. Welling, "Semi-supervised classification with graph convolutional networks," in *ICLR*, 2017.
- [40] W. Aiello, F. Chung, and L. Lu, "A Random Graph Model for Power Law Graphs," in *Experimental Mathematics*, 2001.
- [41] J. Leskovec, "Stanford CS224W: Machine Learning with Graphs," in *cs224w.stanford.edu*.
- [42] C. Morris, N. M. Kriege, F. Bause, K. Kersting, P. Mutzel, and M. Neumann, "TUDataset: A collection of benchmark datasets for learning with graphs," *arXiv preprint arXiv:2007.08663*, 2020.
- [43] P. Holme and B. J. Kim, "Growing scale-free networks with tunable clustering," in *Physical Review E*, 2002.
- [44] Erdős, Pál and Rényi, Alfréd, "On Random Graphs I," in *Publicationes Mathematicae*, 1959.
- [45] Albert, R. and Barabási, L., "Statistical mechanics of complex networks," in *Reviews of Modern Physics*, 2002.
- [46] D. J. Watts and S. H. Strogatz, "Collective dynamics of small-world networks," in *Nature*, 1998.
- [47] E. M. Airoldi, D. M. Blei, S. E. Fienberg, and E. P. Xing, "Mixed Membership Stochastic Blockmodels," in *JMLR*, 2008.
- [48] J. Leskovec, D. Chakrabarti, J. M. Kleinberg, C. Faloutsos, and Z. Ghahramani, "Kronecker Graphs: An Approach to Modeling Networks," in *JMLR*, 2010.
- [49] J. You, R. Ying, X. Ren, W. L. Hamilton, and J. Leskovec, "GraphRNN: Generating Realistic Graphs with Deep Auto-regressive Models," in *ICML*, 2018.
- [50] L. Kong, J. Cui, H. Sun, Y. Zhuang, B. A. Prakash, and C. Zhang, "Autoregressive Diffusion Model for Graph Generation," in *ICML*, 2023.
- [51] A. Bergmeister, K. Martinkus, N. Perraudin, and R. Wattenhofer, "Efficient and Scalable Graph Generation through Iterative Local Expansion," in *ICLR*, 2024.
- [52] Gretton, A., Borgwardt, K. M., Rasch, M. J., Schölkopf, B., and Smola, A., "A kernel two-sample test," in *JMLR*, 2012.
- [53] A. A. Hagberg, D. A. Schult, and P. J. Swart, "Exploring network structure, dynamics, and function using NetworkX," in *SciPy2008*, 2008.